Isme Journal
October 2022, Volume 16 Issue 10 Pages 2398-2405
https://doi.org/10.1038/s41396-022-01289-6
https://archimer.ifremer.fr/doc/00788/89959/

Sinking Trichodesmium fixes nitrogen in the dark ocean

Benavides Mar [1, 2, *], Bonnet Sophie [1], Le Moigne Frédéric A. C. [1, 3], Armin Gabrielle [4], Inomura Keisuke [4], Hallstrøm Søren [5], Riemann Lasse [5], Berman-Frank Ilana [6], Poletti Emilie [1], Garel Marc [1], Grosso Olivier [1], Leblanc Karine [1], Guigue Catherine [1], Tedetti Marc [1], Dupouy Cécile

[1] Aix Marseille Univ, Université de Toulon, CNRS, IRD, MIO UM 110, 13288, Marseille, France
[2] Turing Center for Living Systems, Aix-Marseille University, 13009, Marseille, France
[3] LEMAR, Laboratoire des Sciences de l'Environnement Marin, UMR6539, CNRS, UBO, IFREMER, IRD, 29280, Plouzané, Technopôle Brest-Iroise, France
[4] Graduate School of Oceanography, University of Rhode Island, South Kingstown, RI, USA
[5] Marine Biological Section, Department of Biology, University of Copenhagen, Helsingør, Denmark
[6] Department of Marine Biology, Leon H. Charney School of Marine Sciences, University of Haifa, Mt, Carmel, Haifa, Israel

* Corresponding author : Mar Benavides, email address : mar.benavides@ird.fr

Abstract :

The photosynthetic cyanobacterium Trichodesmium is widely distributed in the surface low latitude ocean where it contributes significantly to N2 fixation and primary productivity. Previous studies found nifH genes and intact Trichodesmium colonies in the sunlight-deprived meso- and bathypelagic layers of the ocean (200–4000 m depth). Yet, the ability of Trichodesmium to fix N2 in the dark ocean has not been explored. We performed 15N2 incubations in sediment traps at 170, 270 and 1000 m at two locations in the South Pacific. Sinking Trichodesmium colonies fixed N2 at similar rates than previously observed in the surface ocean (36–214 fmol N cell−1 d−1). This activity accounted for 40 ± 28% of the bulk N2 fixation rates measured in the traps, indicating that other diazotrophs were also active in the mesopelagic zone. Accordingly, cDNA nifH amplicon sequencing revealed that while Trichodesmium accounted for most of the expressed nifH genes in the traps, other diazotrophs such as Chlorobium and Deltaproteobacteria were also active. Laboratory experiments simulating mesopelagic conditions confirmed that increasing hydrostatic pressure and decreasing temperature reduced but did not completely inhibit N2 fixation in Trichodesmium. Finally, using a cell metabolism model we predict that Trichodesmium uses photosynthesis-derived stored carbon to sustain N2 fixation while sinking into the mesopelagic. We conclude that sinking Trichodesmium provides ammonium, dissolved organic matter and biomass to mesopelagic prokaryotes.

Introduction

Dinitrogen (N_2) fixing prokaryotes (diazotrophs) supply bioavailable nitrogen to planktonic communities, fueling primary production and contributing to carbon export in the ocean [1]. Nitrogen inputs by diazotrophs may become even more important in the future ocean, as global warming enhances water column stratification constraining nitrogen availability for primary producers [2]. Early studies suggested that diazotrophs were only present in low latitude warm oligotrophic waters of the (sub)tropical ocean. However, over the past decade it has become clear that diazotrophs are also found in cold and nutrient-rich environments such as estuaries, shelf seas, polar regions and the ocean's dark pelagic realm [3]. Devoid of light, N_2 fixation in the dark ocean has been attributed to heterotrophic non-cyanobacterial diazotrophs presumably relying on reduced organic compounds for energy and carbon supply [4–6]. However, cyanobacterial diazotrophs have been repeatedly observed in mesopelagic to bathypelagic depths (200 to 4 000 m; Table S1; [7]).

The filamentous cyanobacterium *Trichodesmium* thrives in tropical and subtropical ocean's photic zone where it can introduce 60-80 Tg N y^{-1}, representing roughly half of the reactive nitrogen input to the global ocean [8]. *Trichodesmium* has gas vesicles which confer cells with buoyancy, restricting their vertical distribution in the water column [9, 10]. Accordingly, *Trichodesmium* biomass is thought to be fully remineralized within the photic zone [11]. Recently, however, molecular and imaging studies have documented intact *Trichodesmium* cells and expression of nitrogenase genes down to 4 000 m depth across the world's oceans (Table S1). The mechanisms through which *Trichodesmium* sinks into the dark ocean may include gravitational sinking, downwelling

events [12], mineral ballasting [13], or sudden autocatalytic cell death in response to nutrient limitation [14]. Sinking velocities can be fast enough for surface photoautotrophic cells to reach the dark ocean while remaining viable [15–18], but whether sinking *Trichodesmium* remains metabolically active and carries out N_2 fixation in the dark ocean is not known.

If diazotrophically active *Trichodesmium* fixes N_2 in the dark ocean it would not only affect the global marine nitrogen inventory but conceivably also stimulate microbial processing of particulate organic matter in the (sub)tropical regions where it thrives, affecting vertical carbon export and remineralization in the dark ocean [19]. In the present study we combine $^{15}N_2$ incubation on sediment traps, sinking simulation laboratory experiments and cell metabolism modeling to document that *Trichodesmium* can fix N_2 while sinking far below the photic zone, constituting a hitherto unaccounted reactive nitrogen and organic matter source in the dark ocean.

Materials and Methods

Sinking particle sampling in the South Pacific Ocean

Sinking particles were collected in the western tropical South Pacific during the TONGA cruise (doi: 10.17600/18000884) onboard the R/V *L'Atalante* from November 1st to December 5th 2019. Surface tethered mooring lines (~1 000 m long) were deployed at two stations: S05M (21.157°S, 175.153°W, 5 days) and S10M (19.423°S, 175.133°W, 4 days). The mooring lines featured three sediment traps placed at 170, 270 and 1 000 m. These depth levels were chosen to match the base of the photic layer, the usual depth to

95 calculate flux attenuation (100 m deeper than the photic layer) and the base of the
96 mesopelagic layer, respectively. Each trap consisting of four particle interceptor tubes
97 mounted on an articulated cross-frame. Out of the four tubes deployed per depth, two
98 were used for this study. The first tube was filled with 6 l of 0.2 µm filtered seawater
99 followed by 2.5 l of a 50 g l^{-1} saline brine labeled with $^{15}N_2$ gas. The brine was prepared
100 in a 4.5 l polycarbonate bottle fitted with a septum screwcap and labeled with high-purity
101 $^{15}N_2$ gas (Euroiso-top) injected through the septum and the bubble thoroughly mixed with
102 the brine for several hours using a magnetic stirring plate. The brine had an enrichment
103 ~55 ^{15}N atom % as determined by membrane inlet mass spectrometry [20]. The second
104 tube was filled with 6 l RNAlater solution [21] and 2.5 l of non-labeled brine.
105
106 Immediately upon recovery of the traps onboard, the upper layer of the tubes was
107 carefully removed with a peristaltic pump until the density gradient of the brine was
108 reached. The seawater layer overlying the brine prevented potential intrusions of surface
109 seawater when recovering the trap line onboard. We confirmed that no surface
110 contamination occurred since the particulate organic carbon fluxes measured in brine-
111 filled traps agreed with those measured in parallel traps kept closed during recovery
112 onboard (‘RESPIRE’ traps [22]; M. Bressac, personal communication). The brine of the
113 $^{15}N_2$-labeled traps was transferred to magnetic stirrer plates to ensure homogeneous
114 aliquot sampling. Three aliquots of 50 ml were filtered onto precombusted 25 mm GF/F
115 filters (GE Healthcare, Little Chalfont, UK) for bulk elemental analysis coupled isotope
116 ratio mass spectrometry (EA-IRMS), and another three were filtered onto 1 µm
117 polycarbonate filters (Nucleopore, Whatman, Maidstone, UK) and fixed with 2%
118 microscopy grade paraformaldehyde for single-cell nanoscale secondary ion mass
119 spectrometry (nanoSIMS) analyses (see below). Samples integrating biomass between

2 000 and 200 m (bottlenet [16]) were used to measure natural ^{15}N atom % enrichment of bulk biomass and *Trichodesmium* cells. In parallel, the whole brine volume of the tube filled with RNAlater was immediately filtered onto 0.2 µm polysulfone filters (Supor, Pall Gelman, Port Washington, NY, USA). The filters were transferred to bead beater tubes containing a mix of 0.1 mm and 0.5 mm silica beads, flash-frozen in liquid nitrogen and stored at -80ºC until RNA extractions (see below).

Bulk and Trichodesmium-specific N_2 fixation rates

The $^{15}N/^{14}N$ ratio of dissolved nitrogen was measured by membrane inlet mass spectrometry and the bulk $^{15}N/^{14}N$ ratio and particulate nitrogen concentration of particles with an Integra CN EA-IRMS (SerCon Ltd, Chesire, UK) as described elsewhere [23]. The ^{15}N atom % enrichment of *Trichodesmium* filaments was analyzed on a nanoSIMS 50L (CAMECA, Gennevilliers, France) at the Leibniz Institute for Baltic Sea Research (IOW, Germany). Sample filters were mounted with conductive tape on 10 x 5 mm aluminum stubs (Ted Pella Inc., Redding, CA) and gold-coated to a thickness of ca. 30 nm (Cressington auto sputter coater). A 1 pA 16 keV Cesium (Cs^+) primary beam was scanned on a 512 × 512 pixel raster with a raster area of 15 × 15 µm, and a counting time of 250 µs per pixel. Samples were pre-sputtered with 600 pA Cs^+ current for 2 min in a raster of 30 × 30 µm to remove the gold and surface contaminants and reach the steady state of ion formation. Negative secondary ions $^{12}C^-$, $^{13}C^-$, $^{12}C^{14}N^-$, $^{12}C^{15}N^-$ and $^{31}P^-$ were detected with electron multiplier detectors, and secondary electrons were simultaneously imaged. Sixty serial quantitative secondary ion mass planes were generated, drift corrected and accumulated to the final image. Mass resolving power was >8 000 to resolve isobaric interferences. Data was processed using the

Look@nanoSIMS software [24]. Isotope ratio images were generated by dividing the $^{13}C^-$ ion count by the $^{12}C^-$ ion count, and the $^{12}C^{15}N^-$ ion count by the $^{12}C^{14}N^-$ ion count pixel by pixel. Individual *Trichodesmium* filaments (trichomes) were identified in nanoSIMS secondary electron $^{12}C^-$, $^{12}C^{14}N^-$ images. These images were used to define regions of interest (ROIs). For each ROI, the $^{13}C/^{12}C$ and $^{15}N/^{14}N$ ratios were calculated based on the ion counts averaged over the ROIs.

Bulk N_2 fixation rates were calculated following the equations of Montoya et al. [25]. *Trichodesmium*-specific volumetric N_2 fixation rates were calculated using the following equation:

$$Volumetric\ N_2\ fixation\ rate = \frac{(A_{Tricho} - A_{TrichoNat})}{(A_{N_2} - A_{TrichoNat})} \times \frac{PN_{Tricho}}{t}$$

where A_{Tricho} is the ^{15}N atom% enrichment of individual *Trichodesmium* cells incubated with $^{15}N_2$, $A_{TrichoNat}$ is the natural ^{15}N atom% enrichment of *Trichodesmium* as analyzed by nanoSIMS (see above), A_{N2} is the ^{15}N atom% enrichment of dissolved N_2 measured by membrane inlet mass spectrometry (see above), PN_{Tricho} is the nitrogen biomass of *Trichodesmium* and *t* is the incubation time. PN_{Tricho} is calculated by converting *Trichodesmium nifH* gene copies l^{-1} (as provided by Bonnet et al. [26]) to carbon considering the average of the mmol C : *nifH* ratio provided in Meiler et al. [27]. Carbon is converted to nitrogen considering a C:N ratio of 6:1 [28]. *Trichodesmium* abundance is calculated by converting *Trichodesmium nifH* gene copies l^{-1} into cells l^{-1} considering a ratio of 12 and 103 *nifH* gene copies per *Trichodesmium* cell, obtained empirically for stations S05M and S10M, respectively, by comparing quantitative PCR and microscopy *Trichodesmium* counts [26]. Finally, *Trichodesmium* cell-specific N_2 fixation rates (fmol N

cell^{-1} d^{-1}) are calculated by dividing volumetric rates by *Trichodesmium* abundance (cells l^{-1}).

RNA extractions, nifH gene sequencing and bioinformatics

RNA was extracted using the RNeasy mini kit (Qiagen) including a 1 h on-column DNase digestion. PCRs on extracted RNA controlled for complete DNA digestion. Reverse transcription (RT) were performed with TaqMan Reverse Transcription (Applied Biosystems) using reverse primer nifH3 (5'-ATR TTR TTN GCN GCR TA-3') and 5 µl of RNA extract. Triplicate nested PCR reactions were conducted using degenerate *nifH* primers nifH1 (5'-TGYGAYCCNAARGCNGA-3'write here), nifH2 (5'-ADNGCCATCATYTCNCC-3'), *nifH3* and *nifH4* (5'-TTYTAYGGNAARGGNGG-3') [29]. The PCR mix was composed of 5 µl of 5X MyTaq red PCR buffer (Bioline), 1.25 µl of 25 mM $MgCl_2$, 0.5 µl of 20 µM forward and reverse primers, 0.25 µl Platinum Taq and 5 µl of cDNA (1 µl from the first PCR reaction was used as template in the second reaction). The reaction volume was adjusted to 25 µl with PCR grade water. Triplicate PCR products were pooled and purified using the Geneclean Turbo kit (MP Biomedicals). Samples were sequenced using the Illumina MiSeq platform with 2 × 300 bp paired-end reads. Demultiplexed paired-end sequences were dereplicated, denoised, assembled and chimeras discarded using the DADA2 pipeline [30]. This generated 6 929 ASVs (146 000 ± 18 000 reads per sample). Sequences have been deposited in the Sequence Read Archive under accession number PRJNA742179. The ASVs were translated to amino acid sequences using FrameBot [31] and filtering for homologous genes was done following the NifMAP pipeline [32]. This reduced the number of ASVs to 6 503 accounting for 842 515 reads (96% of all reads). Taxonomic ranks were assigned

195 according to the *nifH* gene reference database collated and maintained by the Zehr
196 research group (v. June 2017; https://www.jzehrlab.com/nifh).
197
198 *Hydrostatic pressure experiments with Trichodesmium cultures*
199
200 The effect of increasing hydrostatic pressure and decreasing temperature on
201 *Trichodesmium* was tested using a sinking particle simulator [33]. Exponentially growing
202 cultures of *Trichodesmium erythraeum* IMS101 grown at 27ºC under a 12h:12 light:dark
203 cycle on YBCII medium [34] were transferred to four autoclaved 500 ml high pressure
204 titanium bottles (HPBs) placed inside incubators (Memmert IPP 750+, Schwabach,
205 Germany) programmed to decrease temperature at the desired pace. For 360 h, the
206 pressure within the HPBs was increased from 0 to 3 MPa using a piloted pressure
207 generator based on a motorized syringe controlled by a computer. Pressure was logged
208 continuously by means of a Metrolog (Metro-Mesures, Mennecy, France) and controlled
209 by the software with a precision of 0.2%. Concomitantly, temperature of the HPBs was
210 decreased from 27 to 14ºC. These conditions simulate those experienced by cells when
211 sinking from the surface to ~300 m depth with a conservative sinking speed of 20 m d^{-1}
212 (at the lower end of empirically measured *Trichodesmium* sinking velocities; Table S2).
213 Triplicate analytical culture aliquots were sampled from two HPBs at 192 and from
214 another two HPBs at 360 h, corresponding to simulated depths of 160 and 300 m,
215 respectively. N_2 fixation incubations at these time points were done under the
216 corresponding hydrostatic pressure conditions by 100 ml culture aliquots to pressurized
217 titanium flasks containing 30% volume of culture medium previously enriched with $^{15}N_2$
218 gas (prepared as explained above) and incubated for 24 h. Particulate and dissolved
219 samples were analyzed by EA-IRMS and MIMS as described above. Cultures under a

12h:12h dark:dark cycle and temperature decrease pace identical to that of pressurized cultures were used as a control.

Sinking Trichodesmium cell metabolism model

We hypothesized that *Trichodesmium* fixes N_2 while sinking into the dark ocean at the expense of carbon accumulated from photosynthesis before starting to sink. Sinking *Trichodesmium* can thus only fix N_2 until reaching the depth where its carbon storage is depleted. To compute how much carbon storage *Trichodesmium* needs to acquire before sinking to be able to fix N_2 at 1 000 m depth, we adapted a previously published coarse-grained cell metabolism model [35]. The model simulates photosynthesis, N_2 fixation, and respiration for the entire trichome, resolving diffusion boundary layers for oxygen transport and distinguishing between photosynthetic and non-photosynthetic cells (Fig. S1). Photosynthetic cells fix carbon with harvested light energy, accumulate carbon, and synthesize new biomass, whereas non-photosynthetic cells use carbon stored by other cells to fix N_2 (Fig. S1).

To adapt the model to *Trichodesmium* colonies sinking into the mesopelagic layer we considered the variability in temperature and oxygen observed from the ocean surface to 1 000 m in our study (Fig. S2) as well as the inhibiting effect of increasing nitrate concentrations on N_2 fixation. Walden's rule [47] was used to simulate the variation of oxygen diffusivity, as in previous studies [37], and the Arrhenius equation was used to simulate the temperature dependencies of metabolisms [35]. The adapted model was applied to *Trichodesmium* sinking from the bottom of the mixed layer (~40 m; Fig. S2) over a wide range of calculated velocities (ranging from 12 to ~600 m d^{-1};

Supplementary Methods) considering a ratio of initial carbon storage level relative to non-storage biomass (R_{Sto}) ranging between 0 and 2. This value of R_{Sto} range is conservative, since it varies between 1 and 10 according to carbohydrate and lipid to protein ratios in various phytoplankton species [38]. To test the effect of nitrate inhibition on *Trichodesmium*'s N_2 fixation in the mesopelagic, we considered a decrease in the diazotrophically active cells by 70 and 50% in each trichome. All model equations are detailed in Inomura et al. [35] and the adapted code is fully available in Zenodo (https://zenodo.org/record/5153594; doi: 10.5281/zenodo.5153594).

Statistical analyses

^{15}N atom % enrichment values were checked for normality using a Shapiro-Wilk test and significant differences between samples tested with Wilcoxon test, using R software package dplyr in RStudio Version 1.2.5033.

Results and Discussion

Trichodesmium fixes N_2 and expresses nifH in the mesopelagic ocean

The isotopic enrichment of single *Trichodesmium* filaments in the traps ranged between 0.428 ± 0.002 and 0.463 ± 0.033 ^{15}N atom % (Fig. 1). The ^{15}N atom % enrichment of all *Trichodesmium* filaments analyzed was significantly higher than that of filaments not incubated with $^{15}N_2$ collected over the same depth range (0.364 ± 0.006 ^{15}N atom %; Wilcoxon test $p = 0.004$ and $p = 0.014$ for S05M and S10M, respectively; Fig. 1). The derived cell-specific N_2 fixation rates ranged between 36 and 214 fmol N cell^{-1} d^{-1} (Table

S3), in the same range of previous *Trichodesmium* cell-specific N_2 fixation measurements in surface waters of the South Pacific [39, 40]. While the salinity in the traps (~50 ppt) was higher than that of ambient waters (~34 ppt), previous studies have shown that increased salinity reduces but does not impair *Trichodesmium* growth up to 42 ppt [41]. Comparing in *Trichodesmium* cultures grown on 34 and 50 ppt showed a decrease in N_2 fixation rates by 63 ± 15 % (Supplementary Methods). Hence, the high salinity of the $^{15}N_2$-labeled brine may have reduced but did not completely inhibit N_2 fixation in *Trichodesmium*, implying that in situ rates could be higher than measured in our traps. Overall, these cell-specific rates indicate that *Trichodesmium* sinking into the mesopelagic zone can fix N_2 at rates comparable to the surface.

Amplicon sequencing revealed that *nifH* gene transcripts annotated as *Trichodesmium* were present in all sediment trap samples, accounting for 26-84% (average 56%) of the sequence reads (Fig. 2). This indicates that *Trichodesmium* constituted a substantial fraction of the diazotroph community that actively transcribed the *nifH* gene in all samples (Fig. 2). However, comparing the $^{15}N_2$ atom % enrichment of bulk sediment trap material and individual filaments, *Trichodesmium* accounted for 1 to 70% of the N_2 fixation activity measured in the traps (Table S3). Hence, other organisms contributed to N_2 fixation within the traps, which could be driven by either surface diazotrophs attached to particles or by true mesopelagic N_2 fixation driven by diazotrophs residing in deep waters. The contribution of *Trichodesmium* to mesopelagic N_2 fixation in the subtropical region studied here is notorious but likely restricted to the (sub)tropical regions where this cyanobacterium abounds. The predicted warming and expansion of oligotrophic subtropical gyres towards higher latitudes may expand the effect of sinking *Trichodesmium* to higher latitudes in the future [42].

Crocosphaera, the only other cyanobacterial group present in the cDNA sequence data, comprised 10% of the cDNA sequence reads of station S05M at 270 m, but less than 0.1% in the other samples. Sequences annotated as the genus *Chlorobium* (Bacteroidota) comprised 60% of cDNA sequences recovered from 1 000 m depth at station S05M and constituted a substantial fraction of the expression profiles of station S10M at 170 m and 270 m, comprising 16% and 20% of cDNA sequences, respectively, but their contribution was less than 1% in the rest of the samples. This indicates that, when specific conditions are met, *Chlorobium* can contribute substantially to the *nifH* transcript pool. A noteworthy contribution to the expression profiles was Alphaproteobacteria classified as the genus *Yangia* (Rhodobacteraceae [43]), which comprised approximately 10% of cDNA sequences of S05M but were virtually undetected at S10M. Both Bacteroidota and Rhodobacteraceae have been identified as epibionts of *Trichodesmium* [44] and were likely attached to the colonies as they sunk from the surface ocean into the traps. The other most prevalent group was Deltaproteobacteria, with genera such as *Desulfatibacillum*, *Desulfobacter*, *Desulfolobus*, and *Desulfovibrio* together comprising 12.5% of cDNA reads on average. This group has not been previously identified as an epibiont of *Trichodesmium* but is commonly observed in sinking particles intercepted with sediment traps in the dark ocean [21].

Sinking Trichodesmium simulation experiments

We confirmed the ability of *Trichodesmium* to fix N_2 under mesopelagic conditions using a particle sinking simulator (see Methods; [42]). *Trichodesmium* cultures submitted to

increasing hydrostatic pressure for 192 and 360 h in the dark (equivalent to 150 and 300 m simulated depth) had ^{15}N atom % enrichment values of 0.375 ± 0.012 and 0.370 ± 0.002 atom %, respectively (Fig. 3A), indicating low but measurable N_2 fixation. Control *Trichodesmium* cultures kept at ambient lab pressure conditions had ^{15}N atom % enrichments of 0.390 ± 0.012 and 0.393 ± 0.008 after 192 and 360 h of incubation, respectively (Fig. 3B). This difference in pressurized (Fig. 3A) and non-pressurized (Fig. 3B) N_2 fixation rates is in agreement with previous metabolic rate slowdown in epipelagic prokaryotes submitted to mesopelagic pressure levels [45] and indicates that increasing pressure reduces but does not completely incapacitate N_2 fixation in *Trichodesmium.* We however note that the while the sinking simulator allows changing pressure and temperature along the simulated sinking process, it does not allow changing nutrient concentrations. The increasing concentrations of nitrate with depth in the mesopelagic may inhibit N_2 fixation. Thus, the rates measured in these sinking simulations represent a non-inhibited upper limit of diazotrophic activity.

How does Trichodesmium obtain energy to fix N_2 at depth?

Trichodesmium uses photosynthetically fixed carbon to fuel the energetically expensive process of N_2 fixation [46]. Hence, the dark conditions of the mesopelagic ocean should be expected to halt photosynthesis and N_2 fixation in *Trichodesmium*, eventually leading to its death. We hypothesized that *Trichodesmium* can fix N_2 in the dark ocean using stored intracellular carbon acquired by photosynthesis before starting to sink. To test how much carbon storage *Trichodesmium* would need to fix N_2 until reaching 1 000 m of depth (corresponding to our field observations), we adapted a published cell metabolism model [47] (Fig. S2). The model simulates changes in intracellular carbon storage (the

345 ratio of carbon storage to biomass or R_{Sto}) while sinking linearly in the water column over
346 a wide range of sinking velocities. The model output provides a relationship between the
347 cell's initial R_{Sto} (R_{Sto} value before starting to sink) and the depth at which carbon storage
348 depletes (Fig. 4).
349
350 Considering that *Trichodesmium* starts sinking below the mixed layer depth (~40 m; Fig.
351 S2), the cell's metabolism becomes dependent on intracellular carbon storage when light
352 is extinguished (~170 m; Fig. S2). Below that depth, R_{Sto} decreases (Fig. 4). When the
353 initial R_{Sto} = 1 (which is at the lower end of the range measured in phytoplankton, see
354 Methods), the cell's carbon storage is depleted at around 750 m assuming a medium
355 sinking velocity of 375 m d^{-1} (yellow dot in Fig. 4). With a higher initial R_{Sto} of 1.3 and the
356 same sinking velocity, carbon storage is depleted at 1 000 m. This suggests that an
357 initial R_{Sto} of at least 1.3 is required for *Trichodesmium* cells to reach 1 000 m of depth
358 with enough carbon to sustain N_2 fixation (pink dot in Fig. 4) and be consistent with our
359 field data (Fig. 1). We also note that *Trichodesmium* may obtain carbon from dissolved
360 organic matter available in their surrounding medium [40], which is not modeled here.
361 This could decrease the required initial *RSto* to sustain N_2 fixation at 1000 m depth.
362
363 *Trichodesmium* invests a significant part of its carbon storage in maintaining low
364 intracellular oxygen concentrations through respiratory protection [47, 48]. The decrease
365 in temperature with depth slows down *Trichodesmium*'s metabolism, decreasing the
366 speed of oxygen diffusion (Walden's rule [47]), which reduces the level of respiratory
367 protection needed to fix N_2 and decreasing and thus carbon storage consumption. While
368 the decrease in temperature with depth also increases the saturated concentration of
369 oxygen, the concentration of oxygen below the mixed layer in our field experiment was

under-saturated (Fig. S2), with oxygen deficit particularly pronounced below 600 m. The combined effects of declining temperatures and oxygen under-saturation contribute to the reduction in carbon storage consumption and are reflected as an increasing slope in the non-linear curve in Fig. 4.

The high nitrate concentrations of the mesopelagic ocean could inhibit N_2 fixation in *Trichodesmium* [49]. While no studies have explicitly tested the inhibition of N_2 fixation by nitrate in the mesopelagic, we explored this effect by considering two constant levels of inhibition (70% and 50%; Fig. S3), which are in the upper range of previous culture and field studies [50]. The model predicts that under 70% and 50% inhibition the required initial R_{Sto} decreases to ~0.5 and ~0.8, respectively (Fig. S3). This indicates that when nitrate inhibits N_2 fixation less carbon storage is consumed, allowing *Trichodesmium* to remain metabolically active at deeper depths (Fig. S3). Previous studies have shown that *Trichodesmium* can fix N_2 in the presence of up to 20 μM nitrate provided phosphate concentrations are high enough to sustain growth [50]. At the depths where traps were deployed during our field experiment, excess phosphate with respect to nitrate according to the Redfield stoichiometry of 16:1 (P* parameter; Fig. S2) likely permitted N_2 fixation (Fig. 1). Finally, the increased partial pressure of CO_2 with depth could also favor N_2 fixation in *Trichodesmium* as previously shown in culture experiments [51].

Is fast sinking necessary for Trichodesmium to fix N_2 in the mesopelagic?

Previous studies have suggested that viable and/or active growing cyanobacteria in the dark ocean are associated with fast-sinking particles, mineral ballasting, or episodic flux

events [17, 18, 52]. While the gas vesicles of *Trichodesmium* may prevent it from sinking, a previous study found that sinking *Trichodesmium* can contribute importantly to organic matter export during atmospheric dust ballasting events [50]. Three months before our cruise, a volcano erupted over the Tonga-Kermadec volcanic arc [53]. This volcano was particularly close to station S10M (~144 km). Measurements of lithogenic silica in the trap material (Supplementary Methods) showed that the lithogenic to particulate organic matter ratio of particulate matter was maximal at station S10M (Table S4). Scanning electron microscopy images (Supplementary Methods) showed volcanic materials intermingled with *Trichodesmium* filaments (Fig. S4), particularly at the 1 000 m trap of station S10M where *Trichodesmium nifH* gene transcripts were more abundant (Fig. 2). Hence, the eruption may have stimulated fast sinking by *Trichodesmium*, particularly at the S10M site. However, both our laboratory sinking simulations and the results of the cell metabolic model indicate that *Trichodesmium* can fix N_2 within the mesopelagic depth range even when sinking at low velocity (e.g. 20 m d^{-1}).

Potential impact of sinking Trichodesmium on mesopelagic prokaryotic communities

Trichodesmium releases up to 19% of the N_2 fixed as ammonium [54], which is the main energy source for dark CO_2 fixation by the abundant Thaumarchaeota [55]. Considering the *Trichodesmium*-specific N_2 fixation rates measured here and a ratio of dark CO_2 fixed per ammonium oxidized of 0.1 [56, 57], the ammonium released by sinking *Trichodesmium* may sustain CO_2 fixation rates of up to 0.2 µmol C m^{-3} d^{-1}. This represents ~13% of previous dark CO_2 fixation rates measured in the mesopelagic ocean [58]. However, to date very few dark CO_2 fixation measurements are available

and their magnitude in *Trichodesmium*-dominated regions (particularly in the South Pacific Ocean) is unknown.

More importantly, *Trichodesmium* releases ca. 50% of its fixed N_2 as dissolved organic nitrogen [59], which mostly composed of labile amino acids [60]. The mycosporine and tryptophan-like compound optical signatures observed at >1 000 m in our study are consistent with previous measurements of natural [61–63] and cultured *Trichodesmium* colonies (Supplementary Methods; Fig. S6). These signals were particularly strong at S10M (Fig. S5) coinciding with highest *Trichodesmium nifH* transcripts (Fig. 2) and supporting the active release of amino acids by sinking *Trichodesmium*. Amino acids released by active sinking *Trichodesmium* could add up to the labile compounds released by sinking particles in the dark ocean [64–67], contributing to the prokaryotic respiration organic matter [68] in the subtropical and tropical regions where *Trichodesmium* occurs.

Conclusions

This study provides the first cell-specific N_2 fixation rates, nitrogenase expression and metabolic mechanistic understanding of *Trichodesmium* sinking into the mesopelagic zone, representing a step forward from early findings of viable surface ocean phytoplankton at depth. Diazotrophically active *Trichodesmium* can provide mesopelagic bacteria and archaea with ammonium and labile amino acids, contributing to chemolithoautotrophy and organic matter remineralization in the mesopelagic zone, respectively. The balance between these two processes sets the ultimate role of the dark ocean in carbon sequestration with consequences for global climate. Given the

widespread blooms of *Trichodesmium* in the surface ocean, which are predicted to expand due to climate change [42], we contend that the impact of sinking *Trichodesmium* on the biogeochemistry of the dark ocean needs to be considered in carbon sequestration models.

Acknowledgments

The authors would like to thank the crew and technical staff of R/V *L'Atalante* as well as the scientists that participated in trap deployment onboard, as well as N. Brouilly and F. Richard at the IBDML SEM facility (Marseille, France). We are indebted to A. Vogts for nanoSIMS analyses (IOW, Warnemünde, Germany) and A. Filella (MIO, Marseille, France) for salinity effect experiments on *Trichodesmium* cultures. This research was supported by Agence Nationale de Recherche grant ANR-18-CE01-0016 (SB), A*Midex grant TONGA (SB), Institut National des Sciences de l'Univers Les Enveloppes Fluides et l'Environnement (INSU-LEFE) grant TONGA (SB), INSU-LEFE grant DEFINE (MB), National Science Foundation EPSCoR Cooperative Agreement OIA-1655221 E (KI) and Danish Council for independent research 6108-00013 (SH and LR). The authors are grateful to M. Sebastián, J.M. Gasol, J. Arístegui and X.A. Álvarez-Salgado for their comments on previous versions of this manuscript.

Competing Interests: Authors declare that they have no competing interests.

Data Availability Statement: All data are available in the main text or the supplementary materials. The model code for this study can be found in

https://zenodo.org/record/5153594 (DOI: 10.5281/zenodo.5153594). Sequences have been deposited in the Sequence Read Archive under accession number PRJNA742179.

References

1. Gruber N, Galloway JN. An Earth-system perspective of the global nitrogen cycle. *Nature* 2008; **451**: 293–296.
2. Hutchins DA, Capone DG. The marine nitrogen cycle: new developments and global change. *Nat Rev Microbiol* 2022.
3. Zehr JP, Capone DG. Changing perspectives in marine nitrogen fixation. *Science* 2020; **368**: eaay9514.
4. Bombar D, Paerl RW, Riemann L. Marine Non-Cyanobacterial Diazotrophs: Moving beyond Molecular Detection. *Trends Microbiol* 2016; **24**: 916–927.
5. Benavides M, Moisander PH, Berthelot H, Dittmar T, Grosso O, Bonnet S. Mesopelagic N2 fixation related to organic matter composition in the Solomon and Bismarck Seas (Southwest Pacific). *PLoS One* 2015; **10**: 1–19.
6. Rahav E, Bar-Zeev E, Ohayon S, Elifantz H, Belkin N, Herut B, et al. Dinitrogen fixation in aphotic oxygenated marine environments. *Front Microbiol* 2013; **4**: 1–11.
7. Benavides M, Bonnet S, Berman-frank I, Riemann L. Deep Into Oceanic N2 Fixation. *Frontiers Marine Science* 2018; **5**: 108.
8. Capone DG, Burns JA, Montoya JP, Subramaniam A, Mahaffey C, Gunderson T, et al. Nitrogen fixation by Trichodesmium spp.: An important source of new nitrogen to the tropical and subtropical North Atlantic Ocean. *Global Biogeochem Cycles* 2005; **19**: 1–17.
9. Villareal TA, Carpenter EJ. Diel buoyancy regulation in the marine diazotrophic cyanobacteria Trichodesmium thiebautii. *Limnol Oceanogr* 1990; **35**: 1832–1837.
10. White AE, Spitz YH, Letelier RM. Modeling carbohydrate ballasting by Trichodesmium spp. *Mar Ecol Prog Ser* 2006.

11. Scharek R, Tupas LM, Karl DM. Diatom fluxes to the deep sea in the oligotrophic North Pacific gyre at Station ALOHA. *Mar Ecol Prog Ser* 1999; **182**: 55–67.
12. Guidi L, Calil PHR, Duhamel S, Björkman KM, Doney SC, Jackson GA, et al. Does eddy-eddy interaction control surface phytoplankton distribution and carbon export in the North Pacific Subtropical Gyre? *Journal of Geophysical Research: Biogeosciences* 2012.
13. Pabortsava K, Lampitt RS, Benson J, Crowe C, McLachlan R, Le Moigne FAC, et al. Carbon sequestration in the deep Atlantic enhanced by Saharan dust. *Nat Geosci* 2017; **10**: 189–194.
14. Bar-Zeev E, Avishay I, Bidle KD, Berman-Frank I. Programmed cell death in the marine cyanobacterium Trichodesmium mediates carbon and nitrogen export. *ISME J* 2013.
15. Smayda TJ. Normal and accelerated sinking of phytoplankton in the sea. *Mar Geol* 1971; **11**: 105–122.
16. Agustí S, González-Gordillo JI, Vaqué D, Estrada M, Cerezo MI, Salazar G, et al. Ubiquitous healthy diatoms in the deep sea confirm deep carbon injection by the biological pump. *Nat Commun* 2015; **6**: 1–8.
17. Sohrin R, Isaji M, Obara Y, Agostini S, Suzuki Y, Hiroe Y, et al. Distribution of Synechococcus in the dark ocean. *Aquat Microb Ecol* 2011; **64**: 1–14.
18. Lochte K, Turley CM. Bacteria and cyanobacteria associated with phytodetritus in the deep sea. *Nature* 1988; **333**: 67–69.
19. Smith DC, Simon M, Alldredge AL, Azam F. Intense hydrolytic enzyme activity on marine aggregates and implications for rapid particle dissolution. *Nature* 1992; **359**: 139–142.

20. Kana TM, Darkangelo C, Hunt MD, Oldham JB, Bennett GE, Cornwell JC. Membrane Inlet Mass Spectrometer for Rapid Environmental Water Samples. *Anal Chem* 1994; **66**: 4166–4170.
21. Fontanez KM, Eppley JM, Samo TJ, Karl DM, DeLong EF. Microbial community structure and function on sinking particles in the North Pacific Subtropical Gyre. *Front Microbiol* 2015; **6**.
22. Boyd PW, McDonnell A, Valdez J, LeFevre D, Gall MP. RESPIRE: An in situ particle interceptor to conduct particle remineralization and microbial dynamics studies in the oceans' Twilight Zone. *Limnol Oceanogr Methods* 2015; **13**: 494–508.
23. Caffin M, Moutin T, Ann Foster R, Bouruet-Aubertot P, Michelangelo Doglioli A, Berthelot H, et al. N2 fixation as a dominant new N source in the western tropical South Pacific Ocean (OUTPACE cruise). *Biogeosciences* 2018.
24. Polerecky L, Adam B, Milucka J, Musat N, Vagner T, Kuypers MMM. Look@NanoSIMS - a tool for the analysis of nanoSIMS data in environmental microbiology. *Environ Microbiol* 2012; **14**: 1009–1023.
25. Montoya JP, Voss M, Kahler P, Capone DG. A Simple, High-Precision, High-Sensitivity Tracer Assay for N2 Fixation. *Appl Environ Microbiol* 1996; **62**: 986–993.
26. Bonnet S, Benavides M, Camps M, Torremocha A, Grosso O, Spungin D, et al. Massive export of diazotrophs across the tropical south Pacific Ocean. *bioRxiv* . 2021. , 2021.05.07.442706
27. Meiler S, Britten GL, Dutkiewicz S, Gradoville MR, Moisander PH, Jahn O, et al. Constraining uncertainties of diazotroph biogeography from nifH gene abundance. *Limnol Oceanogr* 2022.
28. Redfield AC. The influence of organisms on the composition of seawater. *The sea* 1963; **2**: 26–77.

29. Zehr JP, Mellon MT, Zani S. New nitrogen-fixing microorganisms detected in oligotrophic oceans by amplification of nitrogenase (nifH) genes. *Appl Environ Microbiol* 1998; **64**: 3444–3450.
30. Callahan BJ, McMurdie PJ, Rosen MJ, Han AW, Johnson AJA, Holmes SP. DADA2: High-resolution sample inference from Illumina amplicon data. *Nat Methods* 2016; **13**: 581–583.
31. Wang Q, Quensen JFI, Fish JA, Lee TK, Sun Y, Tiedje JM, et al. Ecological patterns of nifH genes in four terrestrial climatic zones Explored with Targeted Metagenomics Using FrameBot, a New Informatics Tool. *MBio* 2013; **4**: 1–9.
32. Angel R, Nepel M, Panhölzl C, Schmidt H, Herbold CW, Eichorst SA, et al. Evaluation of primers targeting the diazotroph functional gene and development of NifMAP - A bioinformatics pipeline for analyzing nifH amplicon data. *Front Microbiol* 2018.
33. Tamburini C, Goutx M, Guigue C, Garel M, Lefèvre D, Charrière B, et al. Effects of hydrostatic pressure on microbial alteration of sinking fecal pellets. *Deep Sea Res Part 2 Top Stud Oceanogr* 2009; **56**: 1533–1546.
34. Chen Y-B, Zehr JP, Mellon M. Growth and nitrogen fixation of the diazotrophic filamentous nonheterocystous cyanobacterium Trichodesmium sp. IMS 101 in defined media: evidence for a circadian rhythm. *J Phycol* 1996; **32**: 916–923.
35. Inomura K, Deutsch C, Wilson ST, Masuda T, Lawrenz E, Sobotka R, et al. Quantifying Oxygen Management and Temperature and Light Dependencies of Nitrogen Fixation by Crocosphaera watsonii. *MSphere* 2019; **4**: 1–15.
36. Fernandez AC, Phillies GDJ. Temperature dependence of the diffusion coefficient of polystyrene latex spheres. *Biopolymers* 1983; **22**: 593–595.

37. Chakraborty S, Andersen KH, Visser AW, Inomura K, Follows MJ, Riemann L. Quantifying nitrogen fixation by heterotrophic bacteria in sinking marine particles. 2–4.
38. Liefer JD, Garg A, Fyfe MH, Irwin AJ, Benner I, Brown CM, et al. The Macromolecular Basis of Phytoplankton C:N:P Under Nitrogen Starvation. *Front Microbiol* 2019; **10**: 763.
39. Berthelot H, Bonnet S, Grosso O, Cornet V, Barani A. Transfer of diazotroph-derived nitrogen towards non-diazotrophic planktonic communities: A comparative study between Trichodesmium erythraeum Crocosphaera watsonii and Cyanothece sp. *Biogeosciences* 2016; **13**: 4005–4021.
40. Benavides M, Berthelot H, Duhamel S, Raimbault P, Bonnet S. Dissolved organic matter uptake by Trichodesmium in the Southwest Pacific. *Sci Rep* 2017; **7**: 1–6.
41. Pade N, Michalik D, Ruth W, Belkin N, Hess WR, Berman-Frank I, et al. Trimethylated homoserine functions as the major compatible solute in the globally significant oceanic cyanobacterium Trichodesmium. *Proc Natl Acad Sci U S A* 2016; **113**: 13191–13196.
42. Boatman TG, Upton GJG, Lawson T, Geider RJ. Projected expansion of Trichodesmium's geographical distribution and increase in growth potential in response to climate change. *Glob Chang Biol* 2020; **26**: 6445–6456.
43. Dai X, Wang B-J, Yang Q-X, Jiao N-Z, Liu S-J. Yangia pacifica gen. nov., sp. nov., a novel member of the Roseobacter clade from coastal sediment of the East China Sea. *Int J Syst Evol Microbiol* 2006; **56**: 529–533.
44. Frischkorn KR, Rouco M, Van Mooy BAS, Dyhrman ST. Epibionts dominate metabolic functional potential of Trichodesmium colonies from the oligotrophic ocean. *ISME J* 2017.

45. Tamburini C, Boutrif M, Garel M, Colwell RR, Deming JW. Prokaryotic responses to hydrostatic pressure in the ocean - a review. *Environ Microbiol* 2013; **15**: 1262–1274.
46. Berman-Frank I, Lundgren P, Chen YB, Küpper H, Kolber Z, Bergman B, et al. Segregation of nitrogen fixation and oxygenic photosynthesis in the marine cyanobacterium Trichodesmium. *Science* 2001; **294**: 1534–1537.
47. Inomura K, Wilson ST, Deutsch C. Mechanistic Model for the Coexistence of Nitrogen Fixation and Photosynthesis in Marine Trichodesmium. *mSystems* 2019; **4**.
48. Berman-Frank I, Lundgren P, Falkowski P. Nitrogen fixation and photosynthetic oxygen evolution in cyanobacteria. *Res Microbiol* 2003; **154**: 157–164.
49. Holl CM, Montoya JP. Interactions between nitrate uptake and nitrogen fixation in continuous cultures of the marine diazotroph Trichodesmium (Cyanobacteria). *J Phycol* 2005; **41**: 1178–1183.
50. Knapp AN. The sensitivity of marine N2 fixation to dissolved inorganic nitrogen. *Front Microbiol* 2012; **3**.
51. Hutchins DA, Fu F-X, Zhang Y, Warner ME, Feng Y, Portune K, et al. CO_2 control of *Trichodesmium* N_2 fixation, photosynthesis, growth rates, and elemental ratios: Implications for past, present, and future ocean biogeochemistry. *Limnol Oceanogr* 2007; **52**: 1293–1304.
52. Karl DM, Church MJ, Dore JE, Letelier RM, Mahaffey C. Predictable and efficient carbon sequestration in the North Pacific Ocean supported by symbiotic nitrogen fixation. *Proceedings of the National Academy of Sciences* 2012.
53. Brandl PA, Schmid F, Augustin N, Grevemeyer I, Arculus RJ, Devey CW, et al. The 6–8 Aug 2019 eruption of 'Volcano F' in the Tofua Arc, Tonga. *J Volcanol Geotherm Res* 2020; **390**: 106695.

54. Mulholland MR, Bronk DA, Capone DG. Dinitrogen fixation and release of ammonium and dissolved organic nitrogen by Trichodesmium IMS101. *Aquat Microb Ecol* 2004; **37**: 85–94.
55. Könneke M, Bernhard AE, De La Torre JR, Walker CB, Waterbury JB, Stahl DA. Isolation of an autotrophic ammonia-oxidizing marine archaeon. *Nature* 2005; **437**: 543–546.
56. Bayer B, Vojvoda J, Reinthaler T, Reyes C, Pinto M, Herndl GJ. Nitrosopumilus adriaticus sp. nov. and Nitrosopumilus piranensis sp. nov., two ammonia-oxidizing archaea from the Adriatic Sea and members of the class Nitrososphaeria. *Int J Syst Evol Microbiol* 2019; **69**: 1892–1902.
57. Baltar F, Herndl GJ. Ideas and perspectives: Is dark carbon fixation relevant for oceanic primary production estimates? *Biogeosciences* 2019; **16**: 3793–3799.
58. Reinthaler T, van Aken HM, Herndl GJ. Major contribution of autotrophy to microbial carbon cycling in the deep North Atlantic's interior. *Deep Sea Res Part 2 Top Stud Oceanogr* 2010; **57**: 1572–1580.
59. Glibert PM, Bronk DA. Release of Dissolved Organic Nitrogen by Marine Diazotrophic Cyanobacteria. *Applied and Environmental Microbiology* 1994; **60**: 3996–4000.
60. Sipler RE, Bronk DA, Seitzinger SP, Lauck RJ, McGuinness LR, Kirkpatrick GJ, et al. Trichodesmium-derived dissolved organic matter is a source of nitrogen capable of supporting the growth of toxic red tide Karenia brevis. *Mar Ecol Prog Ser* 2013; **483**: 31–45.
61. Steinberg DK, Nelson NB, Carlson CA, Prusak AC. Production of chromophoric dissolved organic matter (CDOM) in the open ocean by zooplankton and the colonial cyanobacterium Trichodesmium spp. *Mar Ecol Prog Ser* 2004; **267**: 45–56.

643 62. Subramaniam A, Carpenter EJ, Karentz D, Falkowski PG. Bio-optical properties of
644 the marine diazotrophic cyanobacteriaTrichodesmiumspp. I. Absorption and
645 photosynthetic action spectra. *Limnol Oceanogr* 1999; **44**: 608–617.
646 63. Dias A, Kurian S, Thayapurath S. Optical characteristics of colored dissolved
647 organic matter during blooms of Trichodesmium in the coastal waters off Goa.
648 *Environ Monit Assess* 2020; **192**: 526.
649 64. Seidel M, Vemulapalli SPB, Mathieu D, Dittmar T. Marine Dissolved Organic Matter
650 Shares Thousands of Molecular Formulae Yet Differs Structurally across Major
651 Water Masses. *Environ Sci Technol* 2022.
652 65. Ruiz-González C, Mestre M, Estrada M, Sebastián M, Salazar G, Agustí S, et al.
653 Major imprint of surface plankton on deep ocean prokaryotic structure and activity.
654 *Mol Ecol* 2020; **29**: 1820–1838.
655 66. Turley CM, Mackie PJ. Bacterial and cyanobacterial flux to the deep NE atlantic on
656 sedimenting particles. *Deep Sea Res Part 1 Oceanogr Res Pap* 1995; **42**: 1453–
657 1474.
658 67. Bergauer K, Fernandez-Guerra A, Garcia JAL, Sprenger RR, Stepanauskas R,
659 Pachiadaki MG, et al. Organic matter processing by microbial communities
660 throughout the Atlantic water column as revealed by metaproteomics. *Proc Natl*
661 *Acad Sci U S A* 2018; **115**: E400–E408.
662 68. Herndl GJ, Reinthaler T. Microbial control of the dark end of the biological pump.
663 *Nat Geosci* 2013; **6**: 718–724.
664

Figure legends

Figure 1. *Trichodesmium*-specific ^{15}N atom % enrichment. (A, B) Boxplots showing the range, average and outliers of $^{15}N/^{14}N$ ratios measured in natural (non $^{15}N_2$-labeled) and $^{15}N_2$-labeled samples from 170 m, 270 m and 1 000 m depth at stations S05M and S10M, respectively. The number of trichomes scanned per depth is shown over each box (n values). All *Trichodesmium* filaments analyzed were significantly enriched in ^{15}N. Examples of nanoSIMS $^{15}N/^{14}N$ ratio images of *Trichodesmium* filaments sampled at station S05M showing the $^{15}N/^{14}N$ isotopic ratio enrichment of *Trichodesmium* filaments according to the color bar. Filaments shown in panel (C) are those not incubated with $^{15}N_2$ (natural). The filaments shown in panels (D-F) are those incubated with $^{15}N_2$ and collected from sediment traps deployed at 170, 270 and 1 000 m, respectively. The same pattern is repeated for station S10M in panels (G-J) The scale bar in nanoSIMS $^{15}N/^{14}N$ ratio images is 5 µm.

Figure 2. Diazotroph community expression profiles. Relative abundance of *nifH* cDNA reads originating from sediment traps at 170 m, 270 m, and 1 000 m at stations S05M (A) and S10M (B). Relative abundances were calculated based on 146 000 ± 18 000 reads per sample.

Figure 3. (A) ^{15}N atom % enrichment values of triplicate *Trichodesmium* cultures submitted to a 12h:12h dark:dark light cycle under increasing hydrostatic pressure (0-3 MPa) and decreasing temperature (27 to 14ºC) on a sinking particle simulator for 192 and 360 h (simulating 160 and 300 m depth, respectively). (B) ^{15}N atom % enrichment

689 values of triplicate *Trichodesmium* cultures submitted to a 12h:12h dark:dark at ambient
690 laboratory pressure and decreasing temperature (27 to 14ºC) for 192 and 360 h.
691
692 **Figure 4.** Relationship between the initial carbon storage to biomass ratio (initial R_{Sto}) of
693 *Trichodesmium* cells and the depth at which cell carbon storage is depleted. The x-axis
694 represents the initial R_{Sto}, i.e. the carbon storage to biomass ratio of *Trichodesmium* at
695 40 m (the bottom of the mixing layer, where cells start to sink). The y-axis represents the
696 depletion depth, i.e. the depth at which carbon storage becomes zero. The blue line
697 represents the threshold depth below which cell carbon storage is depleted (and thus N_2
698 fixation is no longer possible) for various initial R_{Sto} values. The shaded area indicates
699 the depletion depth range considering the variability in empirical and theoretical sinking
700 velocities of *Trichodesmium* (Supplementary Methods; Table S2). The yellow and pink
701 dots indicate the depletion depth for initial R_{Sto} values of 1 and 1.3, respectively. The
702 blue line represents the simulation based on the median sinking velocity. The dashed
703 line indicates the depletion depth of 1 000 m depth. The depletion depth must be below
704 1 000 m for cells to fix N_2 at 1000 m depth and explain our field observations.

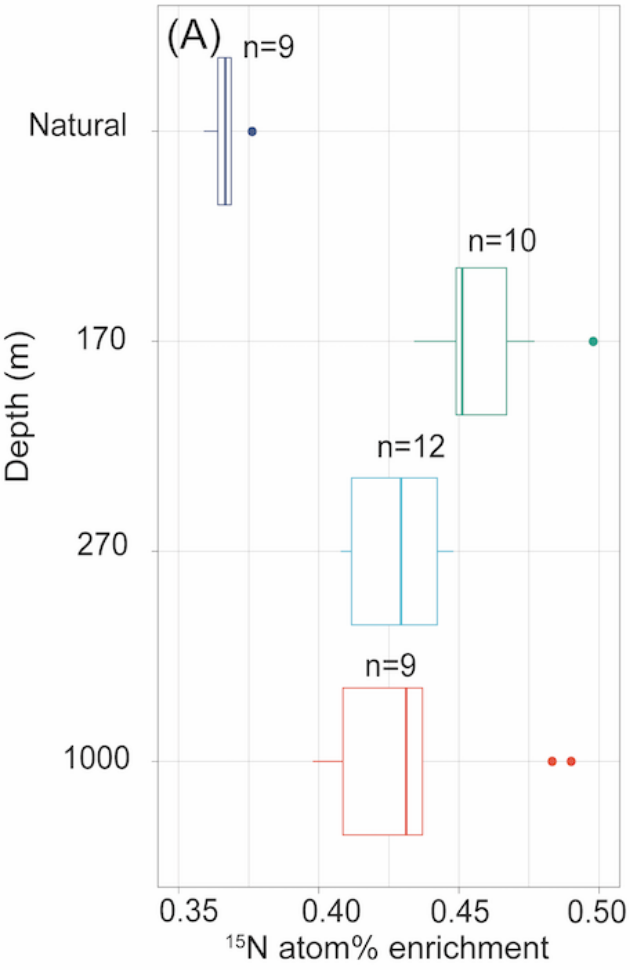
(A)
n=9
Natural
n=10
170
n=12
270
n=9
1000
Depth (m)
0.35
0.40
0.45
0.50
15N atom% enrichment

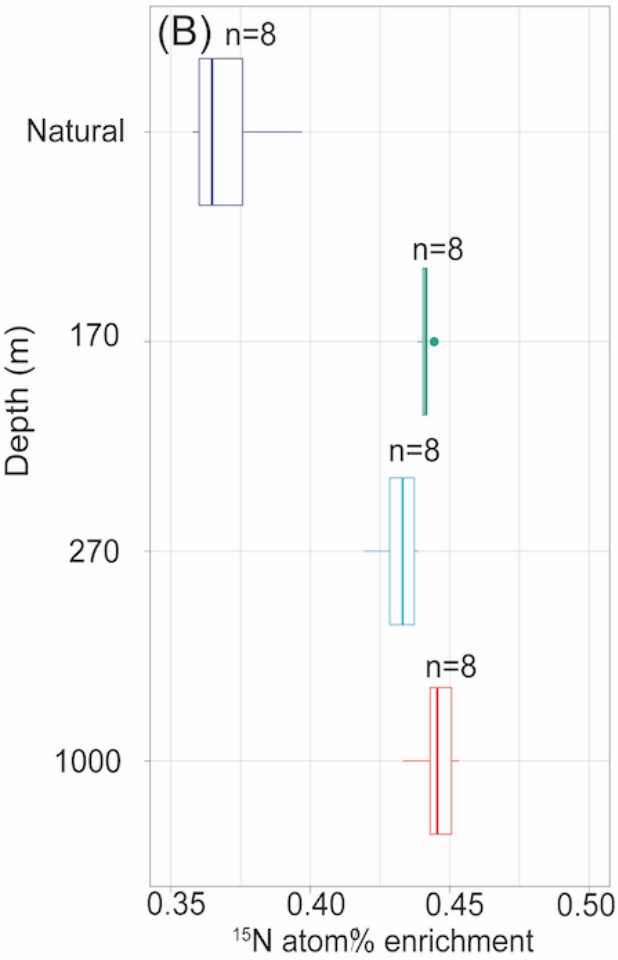
(B)
n=8
Natural
n=8
170
n=8
270
n=8
1000
Depth (m)
0.35
0.40
0.45
0.50
15N atom% enrichment

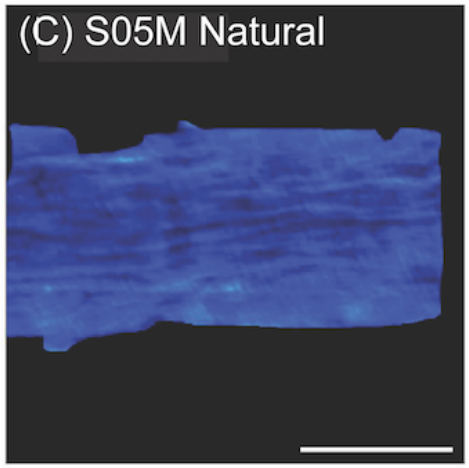
(C) S05M Natural

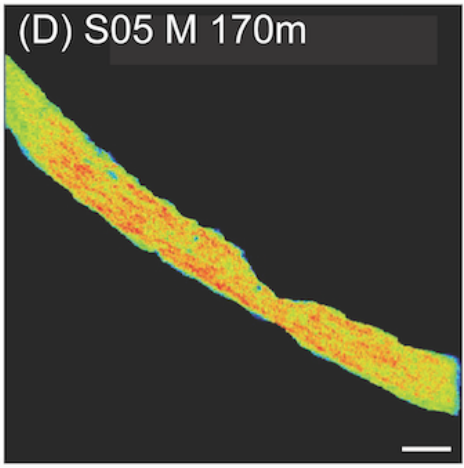
(D) S05 M 170m

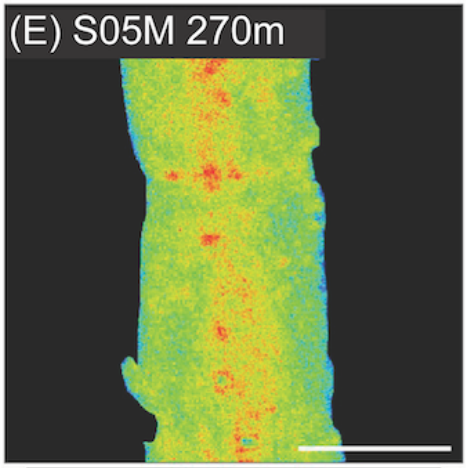
(E) S05M 270m

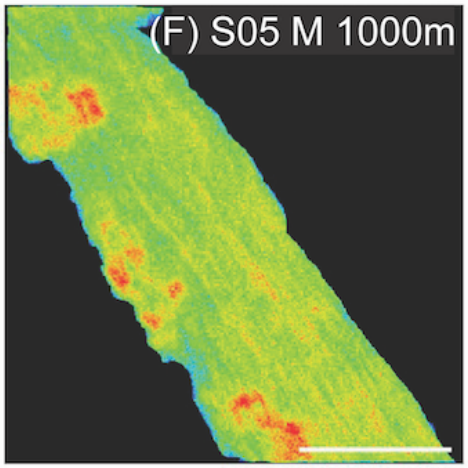
(F) S05 M 1000m

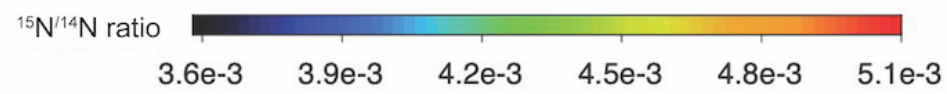
15N/14N ratio
3.6e-3
3.9e-3
4.2e-3
4.5e-3
4.8e-3
5.1e-3

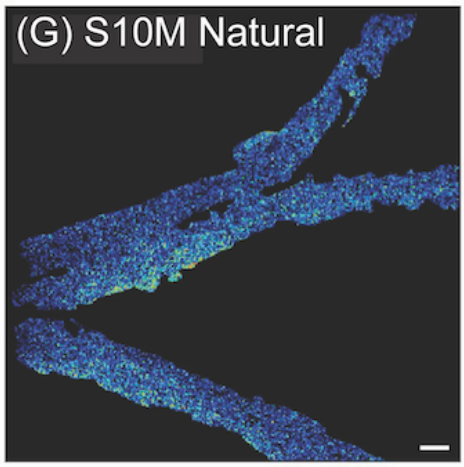
(G) S10M Natural

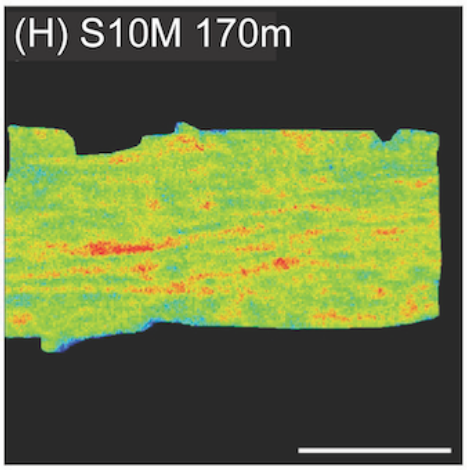
(H) S10M 170m

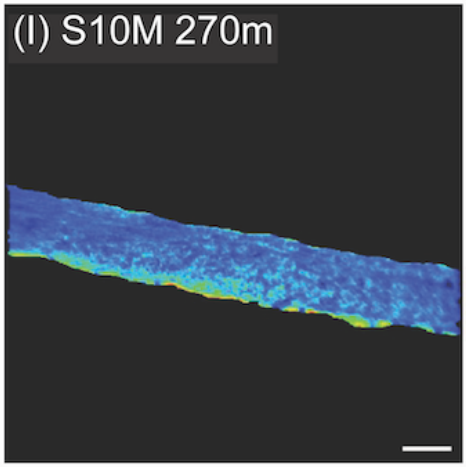
(I) S10M 270m

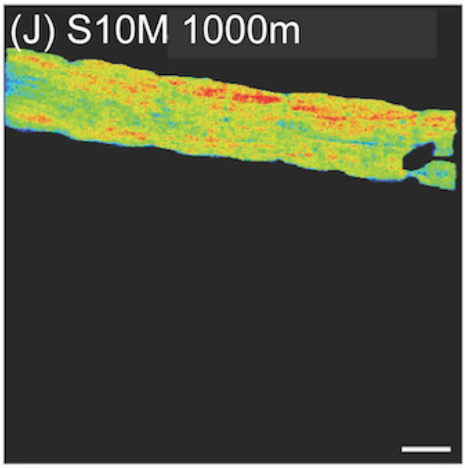
(J) S10M 1000m

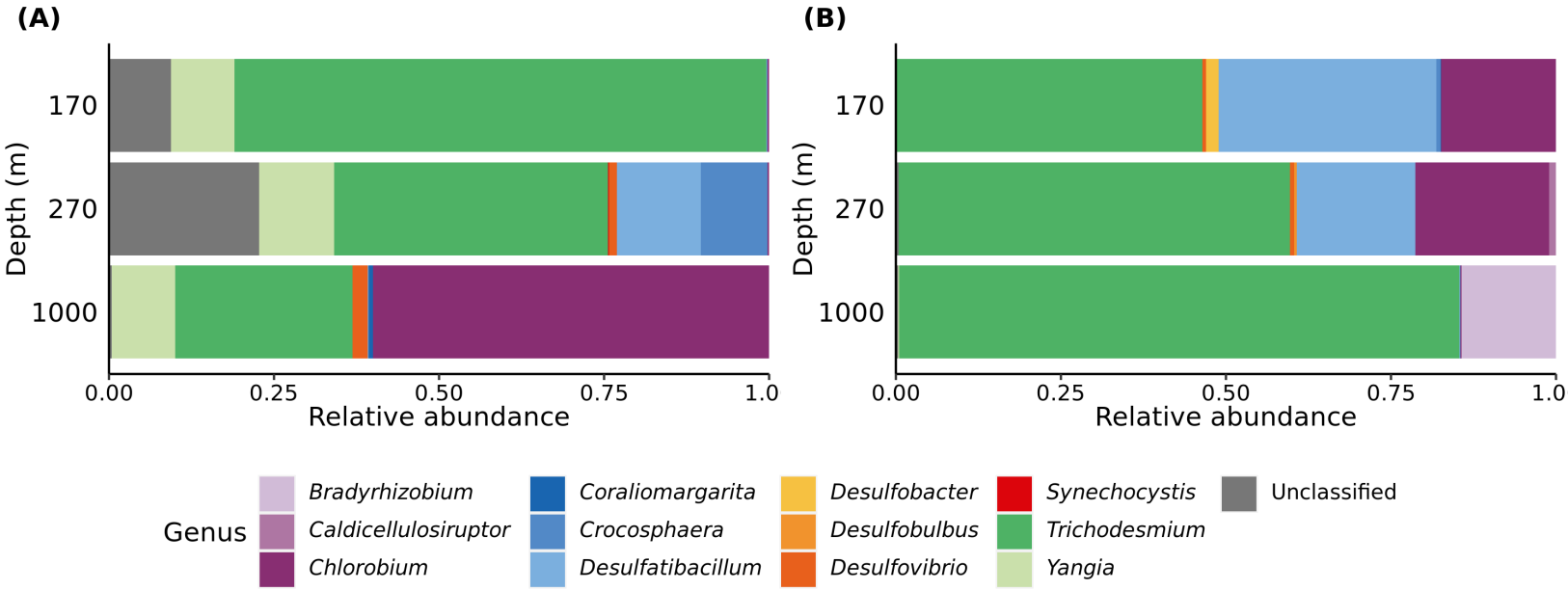
(A)
(B)
Depth (m)
170
270
1000
0.00
0.25
0.50
0.75
1.0
Relative abundance
Genus
Bradyrhizobium
Caldicellulosiruptor
Chlorobium
Coraliomargarita
Crocosphaera
Desulfatibacillum
Desulfobacter
Desulfobulbus
Desulfovibrio
Synechocystis
Trichodesmium
Yangia
Unclassified

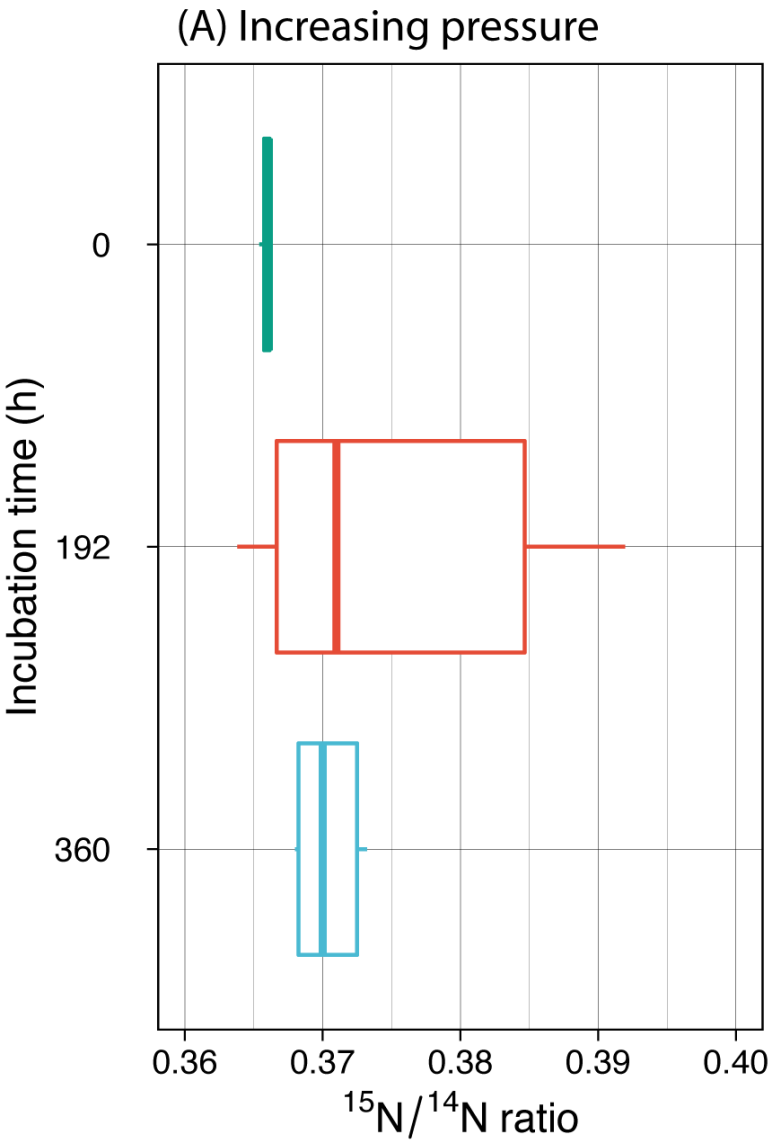
(A) Increasing pressure
Incubation time (h)
0
192
360
0.36
0.37
0.38
0.39
0.40
15N/14N ratio

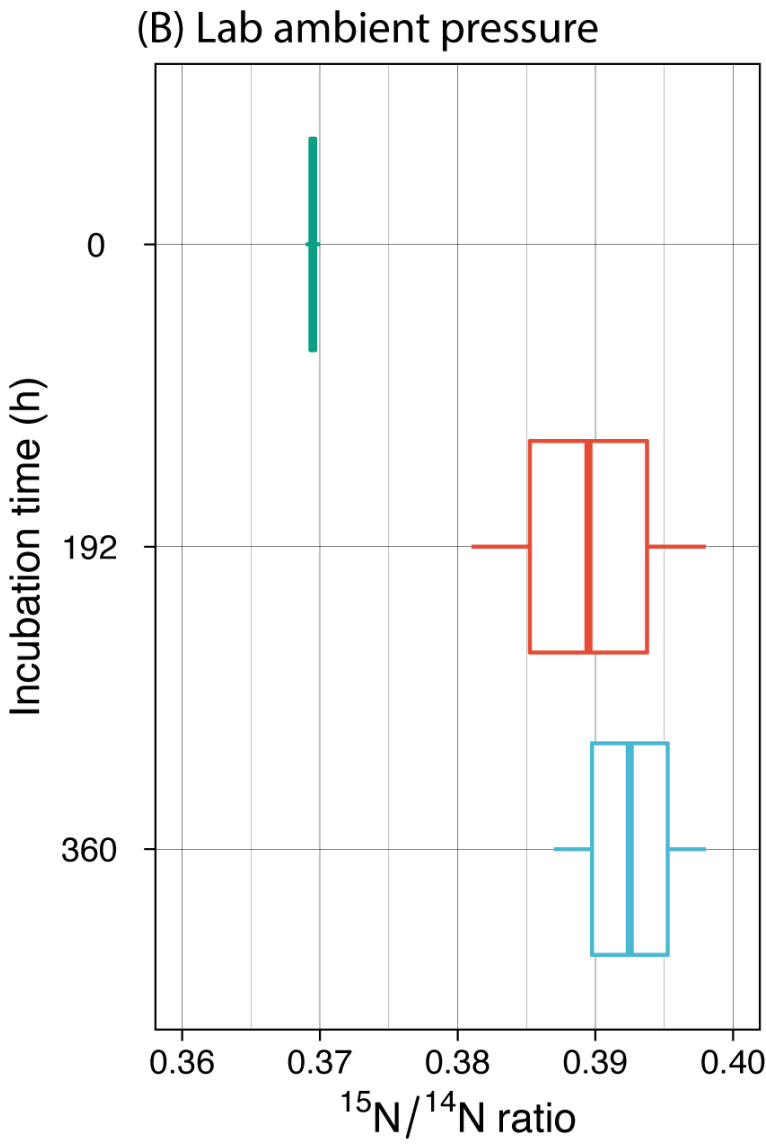
(B) Lab ambient pressure
Incubation time (h)
0
192
360
0.36
0.37
0.38
0.39
0.40
15N/14N ratio

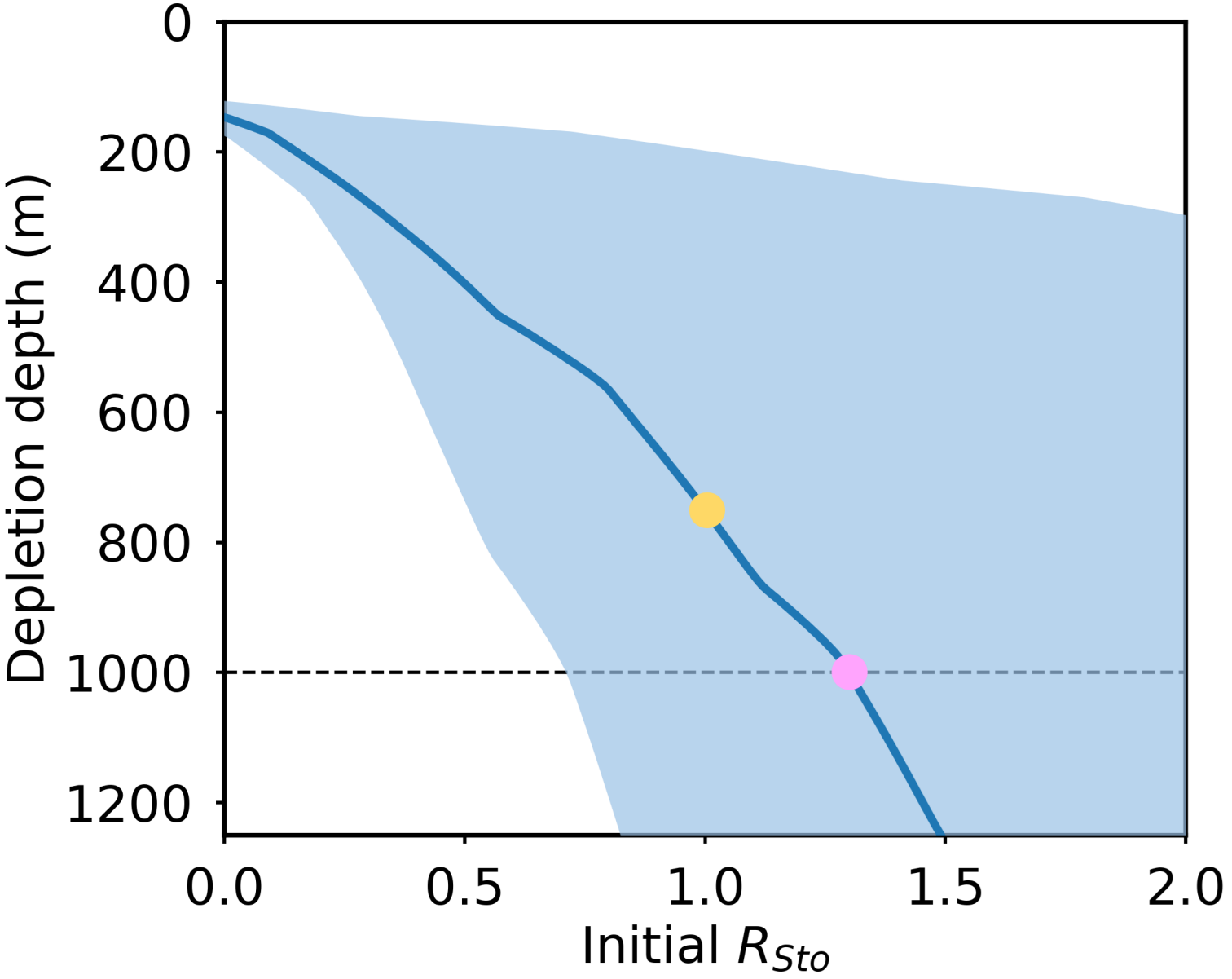
0
200
400
600
800
1000
1200
Depletion depth (m)
0.0
0.5
1.0
1.5
2.0
Initial R_{Sto}